

SEMIANALYTIC FINITE-ELEMENT METHOD IN DYNAMIC PROBLEMS OF LINEAR FRACTURE MECHANICS

V. A. Bazhenov^{1,2}, M. O. Vabishchevich¹, I. I. Solodei^{1,2}, and E. A. Chepurnaya¹

An effective approach to the simulation of crack-type fracture is developed based on the semi-analytical finite element method. Algorithms for determining the parameters of fracture strength for elastic bodies of revolution and prismatic bodies under non-stationary force loading of different intensity and duration are proposed. The energy approach based on the application of a special prismatic and ring finite elements with crack under dynamic loading are used to calculate the fracture parameters. The efficiency of the algorithms is estimated.

Keywords: dynamics, crack, dynamic stress-intensity factor, J-integral, prismatic body, body of revolution, semianalytic finite-element method

Introduction. To extend the service life of critical elements of modern structures, it is important to assess the fracture strength of structural members and components containing cracks or crack-like defects. Structural members are often subjected to non-stationary dynamic loading of different duration and level that can be arbitrarily distributed over the spatial coordinates. The determination of the fracture toughness parameters is very important for adequate assessment of structural strength and accident prevention.

Due to technical difficulties and high cost of experiments in situ, experimental study is extremely complex, if at all possible. Therefore, both deeper theoretical analysis of structural behavior and elaboration of numerical techniques and algorithms for the determination of fracture strength parameters are necessary.

Many equipment components and parts used in mechanical engineering, power engineering, and other fields of technology are actually three-dimensional bodies of revolution or prismatic bodies of complex shape. Different holders, fasteners, damping systems, pressure vessels, and specimens for fracture strength tests, etc. are among them.

The most universal and wide spread numerical method designed for studying such objects is the semi-analytic finite-element method (SAFEM) [3, 6–8]. The principles, modern approaches, and relevant details of numerical techniques elaborated to solve fracture mechanics problems are addressed in [1, 9–11, 13–16]. Numerical algorithms and results of calculation of the stress intensity factor (SIF) for 2D and 3D problems of cracks under static loading have been widely developed.

The aim of the present paper is to further elaborate SAFEM application to problems of fracture mechanics for bodies of revolution and prismatic bodies to analyze transient dynamic processes.

1. Problem Statement. Basic Equations. Let us consider homogeneous isotropic bodies of revolution and prismatic bodies under arbitrary pulse force or kinematic loading over some interval of time.

An orthogonal circular cylindrical system or a Cartesian coordinate system is used to describe the geometrical and mechanical characteristics, initial and boundary conditions, and external loads. This coordinate system is referred to as a basis system further on. The local curvilinear coordinate system associated with the body geometry is introduced to describe the

¹Kyiv National University of Construction and Architecture. ²Scientific Research Institute of Structural Mechanics, 31 Povitroflotsky Av., Kyiv 03037, Ukraine; e-mail: isolodey@gmail.com. Translated from *Prikladnaya Mekhanika*, Vol. 54, No. 5, pp. 35–46, September–October, 2018. Original article submitted October 22, 2016.

stress–strain state (SSS) of the complex-shaped body. It is assumed that the components of the transformation tensor between the local and basis coordinate systems are known at each point of the body [5]:

$$c_{,j}^{i'} = \frac{\partial Z^{i'}}{\partial x^j}, \quad x_{,j'}^i = \frac{\partial x^i}{\partial Z^{j'}}, \quad g_{ij} = c_{,i}^{m'} c_{,j}^{n'} g_{mn}, \quad g^{ij} = \frac{A(g_{ij})}{g}.$$

Further on, the Latin sub- and superscripts take the values 1, 2, and 3 while the Greek sub- and superscripts take the values 1 and 2; the comma placed before the subscript denotes differentiation; $A(g_{ij})$ is the algebraic complement of the element g_{ij} , $g = \det[g_{ij}]$ is the determinant of the matrix.

The nonzero components of the metric tensor specifying the basis vector scales are of the form

$$g_{11'} = g_{22'} = 1, \quad g_{33'} = (Z^{2'})^2,$$

for the orthogonal cylindrical coordinate system and

$$g_{11'} = g_{22'} = g_{33'} = 1$$

for Cartesian coordinate system.

The nonzero Christoffel symbols of the second kind $\Gamma_{l'm'}^{k'}$, in the orthogonal cylindrical coordinate system are expressed as

$$\Gamma_{33'}^{2'} = -Z^{2'}, \quad \Gamma_{32'}^{3'} = \Gamma_{23'}^{3'} = \frac{1}{Z^{2'}},$$

while they become zero in the Cartesian coordinate system:

$$\Gamma_{l'm'}^{k'} = 0.$$

The components of the strain tensor in the local coordinate system are expressed in terms of the displacements $u_{k'}$, in the basis coordinate system as follows:

$$\varepsilon_{ij} = \frac{1}{2} (u_{k',i} c_{,j}^{k'} + u_{k',j} c_{,i}^{k'}) - u_{k'} c_{,i}^{m'} c_{,j}^{n'} \Gamma_{mn}^{k'}. \quad (1)$$

The components of the stress tensor in the local coordinate system are determined in terms of the strain components based on the generalized Hooke's law [5]:

$$\sigma^{ij} = d^{ijkl} \varepsilon_{kl}, \quad d^{ijkl} = \lambda g^{ij} g^{kl} + \mu (g^{jl} g^{ik} + g^{il} g^{jk}).$$

At an arbitrary moment, the elastic strain state satisfies the equation of motion

$$\int_V \rho \ddot{u}^{i'} \delta u_i dV + \int_V \sigma^{ij} \delta \varepsilon_{ij} dV - \int_V f^{i'} \delta u_i dV - \int_{S_p} p^{i'} \delta u_i dS = 0$$

according to the Lagrange–d'Alembert principle.

The initial conditions are set as displacement and velocity distributions at some fixed moment t_0 chosen to be the time coordinate origin, i.e., $u(Z^{i'}, t_0) = u_0(Z^{i'})$, $\dot{u}(Z^{i'}, t_0) = \dot{u}_0(Z^{i'})$, $Z^{i'} \in V$.

It is also assumed that the kinematic boundary conditions $u(Z^{i'}, t) = \tilde{u}(Z^{i'}, t)$ are set on the part S_u of the surface ($Z^{i'} \in S_u$) while the system of loads arbitrarily oriented in space and time is set on the part S_p of the surface having the normal $\bar{n} = n_j e^j$:

$$z_{,i}^{k'} \sigma^{ij} n_j = \tilde{p}(Z^{k'}, t), \quad Z^{k'} \in S_p.$$

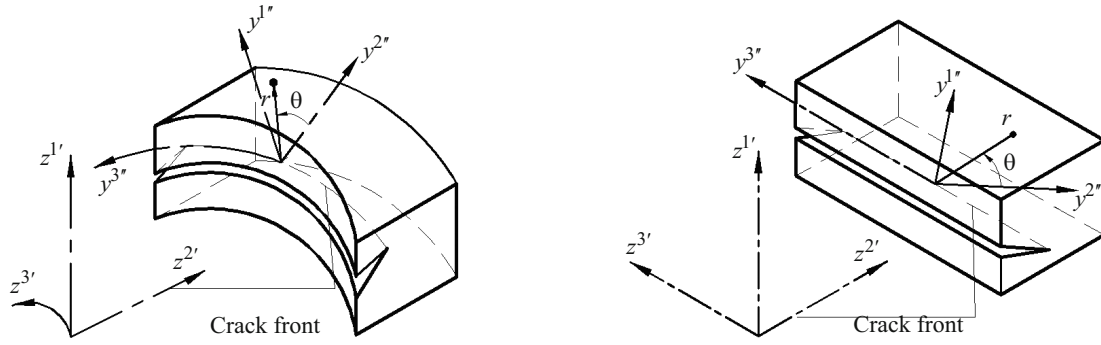


Fig. 1

For the cases of rectilinear prismatic bodies and bodies of revolution, let us consider a crack with front having the same direction as the body generatrix. The portions of the bodies containing the crack are shown in Fig. 1.

There are three types of cracks: normal tear, in-plane shear, and antiplane shear. The formulas relating the components of the stress tensor and the displacement vector and the dynamic stress intensity factor (SIF) depend on the crack opening mode as follows:

normal tear crack opening (mode I):

$$\sigma^{i''j''}(t) = K_I(t) H_I^{i''j''}(r, \theta), \quad i'', j'' = 1, 2, \quad (2)$$

$$u_{i''}(t) = K_I(t) H_I^{i''}(r, \theta), \quad (3)$$

in-plane shear crack opening (mode II):

$$\sigma^{i''j''}(t) = K_{II}(t) H_{II}^{i''j''}(r, \theta), \quad i'', j'' = 1, 2, \quad (4)$$

$$u_{i''}(t) = K_{II}(t) H_{II}^{i''}(r, \theta), \quad (5)$$

antiplane shear crack opening (mode III):

$$\sigma^{i''j''}(t) = K_{III}(t) H_{III}^{i''j''}(r, \theta), \quad i'', j'' = 1, 3, \quad (6)$$

$$u_{i''}(t) = K_{III}(t) H_{III}^{i''}(r, \theta), \quad (7)$$

where H are known functions of the asymptotic formulas for the components of the stress tensor and displacement vector in the vicinity of the crack tip [13].

To define the J-integral for a dynamic problem, the following formula is used:

$$J_k(t) = \frac{1}{\Delta} \lim_{\varepsilon \rightarrow 0} \int_{S_\varepsilon} \left[\{W(t) + T(t)\} n_{(3-k)} - \sigma^{ij}(t) \frac{\partial u_i(t)}{\partial y^{(3-k)''}} n_j \right] dS \quad (k = 1, 2), \quad (8)$$

where W and T are the potential and kinetic energies, respectively; S_ε is the surface of a small volume around the crack front segment (Fig. 2) of length Δ ; n_j are the components of the outer normal to the surface F ; u_i and σ^{ij} are the displacements and

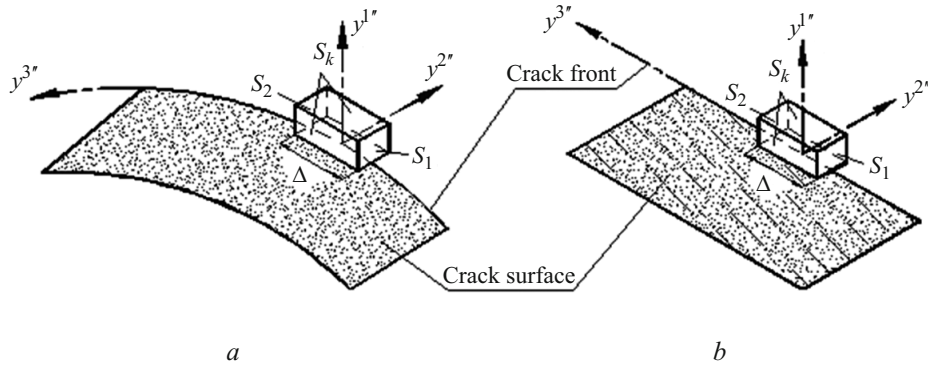


Fig. 2

stresses, respectively; $y^{i'}$ is the local coordinate system attached to the crack. The segment of the crack front for the body of revolution and rectilinear prismatic body is shown in Figs. 2a and 2b.

For convenience, the time index is omitted further on. According to [13], there is the following relation between the SIF and J-integral:

$$J_1 = \frac{1}{H} (K_I^2 + K_{II}^2) + \frac{1}{2\mu} K_{III}^2, \quad J_2 = -\frac{2}{H} K_I K_{II},$$

where $J_1 = G_I + G_{II} + G_{III}$, and G_I, G_{II}, G_{III} are the elastic energy release rates.

It is worth mentioning here that

$$K_I = \sqrt{\tilde{E}G_I}, \quad K_{II} = \sqrt{\tilde{E}G_{II}}, \quad K_{III} = \sqrt{2\mu G_{III}} \quad \text{or}$$

$$K_{I/II} = \frac{1}{2} \sqrt{\tilde{E}} (\sqrt{J_1 - J_2 - G_{III}} \pm \sqrt{J_1 + J_2 - G_{III}}),$$

where $\tilde{E} = E$ for plane stress and $\tilde{E} = E / (1 - \nu^2)$ for plane strain.

To simulate the crack, a thin contact layer is introduced. Within the layer, the stress–strain state (SSS) is described referring to the additional coordinate system $y^{i'}$ associated with the crack front configuration (Fig. 3). The thickness of the FE layer has to satisfy the following two conditions: (i) the layer thickness should be small enough compared to the body (because this layer is actually a dummy layer introduced in order to ease the numerical simulation of the crack) and (ii) the computation stability depends significantly on the FE dimension ratio.

Let us consider special prismatic (Fig. 3a) and circular closed (Fig. 3b) FEs with arbitrary curvilinear rectangular cross section containing the crack (Fig. 3). It is assumed that the element region is transformed to a unit square with internal properties defined by the mechanical and geometrical characteristics of the FE.

Special finite elements with crack (SpFEC) are developed on the basis of SAFEM using circular closed and prismatic FEs [12].

The additional conditions $\sigma^{1'1'} \leq 0$, $\sigma^{1'2'} = 0$, $\sigma^{1'3'} = 0$ have to be met to take into account the crack segment intersecting the element cross section.

To solve the dynamic problems for the body with crack, it is necessary to introduce some restrictions on the equations of motion to prevent the mutual penetration of the crack edges $\sigma^{1'1'} \leq 0$ because positive and negative forces are involved in the solution of nonstationary problems. The same situation occurs in static problems (for instance, in the problem of bending of a plate containing a through crack with edges tending to open on the stretched surface and to close on the compressed surface of the plate). This can be easily treated in the frame of SpFEC by the variation of the stress $\sigma^{1'1'}$ which is normal to the contact surface of the crack edges.

The tensor of elastic constants $\sigma^{mn} = d_*^{mnst} \varepsilon_{st}$ should be corrected to provide zero stress on the crack surface.

The components of the correcting terms for the tensor of elastic constants

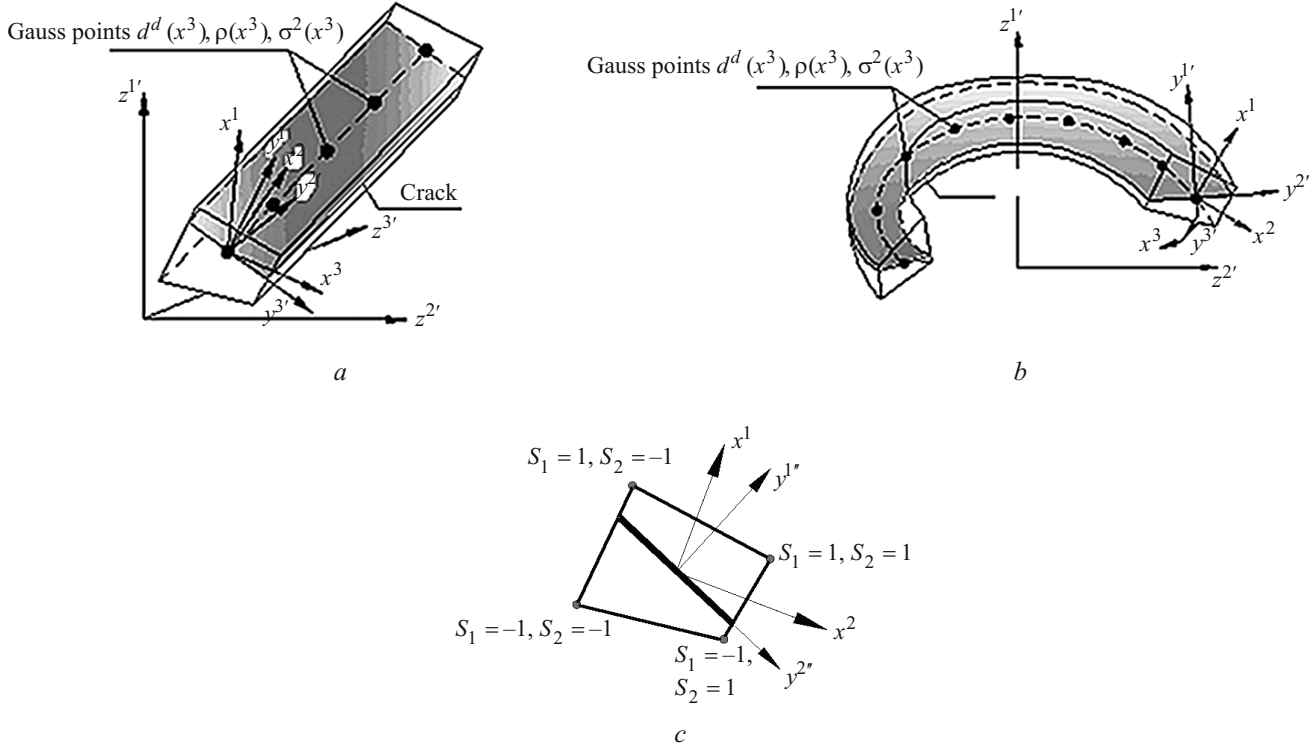


Fig. 3

$$d_*^{mnst} = d^{mnst} - d_p^{mnst} - d_c^{mnst} - d_q^{mnst} \quad (9)$$

are determined by the Lamé coefficients and transformation tensors governing the relations between the basis coordinate system $Z^{i'}$ and the crack coordinate system $y^{i'}$:

$$d_p^{mnst} = \frac{2\mu}{1 + \lambda/2\mu} S^{mn} S^{st}, \quad S^{mn} = \frac{\lambda}{2\mu} g^{mn} + c_{1r}^m c_{1r}^n,$$

$$d_c^{mnst} = \mu(r_1^{ns} r_2^{mt} + r_1^{ms} r_2^{nt} + r_1^{nt} r_2^{ms} + r_1^{mt} r_2^{ns}), \quad d_q^{mnst} = \mu(r_1^{ns} r_3^{mt} + r_1^{ms} r_3^{nt} + r_1^{nt} r_3^{ms} + r_1^{mt} r_3^{ns}),$$

$$c_{i^*}^m = c_{k^*}^m c_{i^*}^{k^*}, \quad r_{i^*}^{ms} = c_{(i)}^m c_{(i)}^s, \quad c_{k^*}^m = \partial x^m / \partial Z^{k^*}, \quad c_{i^*}^{k^*} = \cos \beta, \quad \beta \equiv (Z^{k^*} \wedge y^{i^*}),$$

where the coefficients $c_{3^*}^\alpha = c_\alpha^3 = 0$, $c_{3^*}^3 = 1$ for the bodies of revolution, and $c_{3^*}^\alpha = c_\alpha^3 = 0$, $c_{3^*}^3 = 1/a$ for the prismatic bodies.

In fact, the approach being elaborated is based on a special modification of the physical and mechanical properties of the material. An important advantage of the approach is the approximation of the system of deformable solids by a single body using special FEs. Moreover, the effective stiffness matrix for the special FE is calculated by the same formulas as for the standard FE with the only correction needed for the elements of the elastic constant matrix.

Note that the circular FE is closed and its geometrical parameters are constant along the circumference. Accounting for these two facts and satisfying the boundary conditions for hinged prismatic bodies, we approximate the unknown distributions (displacements, velocities, and accelerations) along the x^3 -direction (see Fig. 3) and their node values are approximated by 2π -periodic functions of x^3 and by truncated trigonometric Fourier series, respectively:

$$(u : \dot{u} : \ddot{u})_{k'(S_1, S_2)} = \sum_{l=l_0}^L (u : \dot{u} : \ddot{u})_{k'(S_1, S_2)}^l \Psi_{(k')}^l, \quad (10)$$

where $\psi_{1'}^l = \psi_{2'}^l = \cos lx^3$, $\psi_{3'}^l = \sin lx^3$, $l_0 = 0$, $0 \leq x^3 \leq 2\pi$ for the circular FE and $\psi_{1'}^l = \psi_{2'}^l = \sin \frac{\pi l}{2} x^3$, $\psi_{3'}^l = \cos \frac{\pi l}{2} x^3$, $l_0 = 1$, $0 \leq x^3 \leq 2$ for the prismatic FE.

The components of the strain and stress tensors at the center of the FE are defined as follows:

$$\begin{aligned}
\overset{\circ}{\varepsilon}_{ij} &= \sum_{l=l_0}^L \overset{\circ}{\bar{\varepsilon}}_{ij}^l \psi_{1'}^l + \overset{\circ}{\bar{\varepsilon}}_{ij}^l \psi_{3'}^l, & \overset{\circ}{\varepsilon}_{ij,\alpha} &= \sum_{l=l_0}^L \overset{\circ}{\bar{\varepsilon}}_{ij,\alpha}^l \psi_{1'}^l + \overset{\circ}{\bar{\varepsilon}}_{ij,\alpha}^l \psi_{3'}^l, \\
\overset{\circ}{\bar{\varepsilon}}_{ij}^l &= l \bar{B}_{ij}^{k'(S_1, S_2)} u_{k'(S_1, S_2)}^l, & \overset{\circ}{\bar{\varepsilon}}_{ij,\alpha}^l &= l \bar{B}_{ij,\alpha}^{k'(S_1, S_2)} u_{k'(S_1, S_2)}^l, \\
\overset{\circ}{\bar{\varepsilon}}_{ij}^l &= l \bar{B}_{ij}^{k'(S_1, S_2)} u_{k'(S_1, S_2)}^l, & \overset{\circ}{\bar{\varepsilon}}_{ij,\alpha}^l &= l \bar{B}_{ij,\alpha}^{k'(S_1, S_2)} u_{k'(S_1, S_2)}^l, \\
\overset{\circ}{\sigma}^{ij} &= \sum_{l=l_0}^L \overset{\circ}{\bar{\sigma}}_l^{ij} \psi_{1'}^l + \overset{\circ}{\bar{\sigma}}_l^{ij} \psi_{3'}^l, & \overset{\circ}{\sigma}^{ij,\alpha} &= \sum_{l=l_0}^L \overset{\circ}{\bar{\sigma}}_{,\alpha l}^{ij} \psi_{1'}^l + \overset{\circ}{\bar{\sigma}}_{,\alpha l}^{ij} \psi_{3'}^l, \\
\overset{\circ}{\bar{\sigma}}_l^{ij} &= d^{ijkm} \overset{\circ}{\bar{\varepsilon}}_{km}^l, & \overset{\circ}{\bar{\sigma}}_{,\alpha l}^{ij} &= d^{ijkm} \overset{\circ}{\bar{\varepsilon}}_{km}^l, & \overset{\circ}{\bar{\sigma}}_l^{ij} &= d^{ijkm} \overset{\circ}{\bar{\varepsilon}}_{km}^l, & \overset{\circ}{\bar{\sigma}}_{,\alpha l}^{ij} &= d^{ijkm} \overset{\circ}{\bar{\varepsilon}}_{km}^l.
\end{aligned} \tag{11}$$

The coefficients of the matrices $[B]$ are calculated using formulas (1) and expansions (10).

To derive the generalized amplitude stiffness matrix for the FE of two types, the following expression for the potential energy variation is used:

$$\delta W = \iiint_{x^1 x^2 x^3} \sigma^{ij} \delta \varepsilon_{ij} \sqrt{g} dx^1 dx^2 dx^3.$$

Expanding the components of the strain and stress tensors into Maclaurin series and integrating over x^1 and x^2 yields

$$\delta W = \int_{x^3} \left(\sigma^{ij} \delta \varepsilon_{ij} + \frac{1}{12} \sum_{\alpha=1}^2 \sigma_{,\alpha}^{ij} \delta \varepsilon_{ij,\alpha} \right) \sqrt{g} dx^3$$

considering the fact that the stress expansion coefficients are related to the strain increment expansion coefficients by Hooke's law.

Using the relation between the expansions coefficients of strain increment and displacement, the expression for the FE energy variation can be rewritten in terms of amplitudes (using the Fourier series) as follows:

$$\delta W = \sum_{l=l_0}^L \delta W_l, \quad \delta W_l = \left[\overset{\circ}{\bar{\sigma}}_l^{ij} \delta \overset{\circ}{\bar{\varepsilon}}_{ij}^l + \overset{\circ}{\bar{\sigma}}_l^{ij} \delta \overset{\circ}{\bar{\varepsilon}}_{ij}^l + \frac{1}{12} \sum_{\alpha=1}^2 (\overset{\circ}{\bar{\sigma}}_{,\alpha l}^{ij} \delta \overset{\circ}{\bar{\varepsilon}}_{ij,\alpha}^l + \overset{\circ}{\bar{\sigma}}_{,\alpha l}^{ij} \delta \overset{\circ}{\bar{\varepsilon}}_{ij,\alpha}^l) \right] \sqrt{g}.$$

Numerical integration with over x^3 yields the generalized amplitude stiffness matrix for both FEs in the form

$$[K]_{ll} = \left[\sum_{\beta=1}^2 [B_\beta]_l^T [D_\beta] [B_\beta]_l + \frac{1}{12} \sum_{\alpha=1}^2 [B_\beta]_{\alpha l}^T [D_\beta]_{\alpha} [B_\beta]_{\alpha l} \right] \sqrt{g}.$$

The matrix $[D_\beta]$ should be modified according to expression (9).

Kinetic energy variation in the local coordinate system is expressed as

$$\delta T = \int_{x^1} \int_{x^2} \int_{x^3} \rho \ddot{u}^{k'} \delta u_{k'} \sqrt{g} dx^1 dx^2 dx^3.$$

Averaging the mass near a node on the assumption that each nodal mass represents a part of the masses of the FEs adjoining this given node, we rearrange the kinetic energy variation as

$$\delta T = \frac{1}{4} \int_{x^3} \rho \ddot{u}^{k'} \delta u_{k'} \sqrt{g} dx^3.$$

Using (10), we get

$$\delta T = \sum_{l=l_0}^L \delta T_l,$$

$$\text{where } \delta T_l = \frac{1}{4} \rho \ddot{u}_{k'(S_1, S_2)}^l \delta u_{k'(S_1, S_2)}^l g_{(S_1, S_2)}^{kk'} \sqrt{g}.$$

Then the expression for the generalized amplitude mass matrix becomes

$$[M]_{ll} = \frac{1}{4} \rho \sqrt{g} [g^{kk'}].$$

The Newmark method or the normal mode expansion method modifications written for SAFEM amplitude subsystems are used for time integration of the equations of motion.

A distinctive feature of the SAFEM is that the amplitudes of the displacement vector, velocity, and acceleration components are chosen as unknowns. Moreover, determination of the amplitudes for homogeneous bodies along the directrix reduces to solving the following system of independent differential equations of the second order at each moment τ :

$$[M]_{ll} \ddot{\mathcal{U}}\}^{l, \tau} + [K]_{ll}^{\tau} \mathcal{U}\}^{l, \tau} = \mathcal{Q}\}^{\tau} \quad (l = l_0, \dots, L), \quad (12)$$

where $\mathcal{Q}\}$ is the force vector which is determined by varying the work done by the internal and external forces.

Following the Newmark method [4], the unknown displacement and velocity amplitudes at the moment $t + \Delta t$ are expressed using the same parameter values at the previous time step according to the finite difference formulas

$$[\tilde{K}]_{ll}^{t+\Delta t} \mathcal{U}\}^{l, t+\Delta t} = \tilde{\mathcal{Q}}\}_l^{t+\Delta t},$$

$$\text{where } [\tilde{K}]_{ll}^{t+\Delta t} = [K]_{ll}^{t+\Delta t} + a_0 [M]_{ll}, \quad \tilde{\mathcal{Q}}\}_l^{t+\Delta t} = \mathcal{Q}\}_l^{t+\Delta t} + [M]_{ll} a_0 \mathcal{U}\}^{l, t} + a_2 \dot{\mathcal{U}}\}^{l, t} + a_3 \ddot{\mathcal{U}}\}^{l, t}.$$

Solving the system of equations yields the displacement amplitudes at $t + \Delta t$ which are used to calculate the velocity and acceleration amplitudes at the same moment $t + \Delta t$:

$$\ddot{\mathcal{U}}\}^{l, t+\Delta t} = a_0 (\mathcal{U}\}^{l, t+\Delta t} - \mathcal{U}\}^{l, t}) - a_2 \dot{\mathcal{U}}\}^{l, t} - a_3 \ddot{\mathcal{U}}\}^{l, t},$$

$$\dot{\mathcal{U}}\}^{l, t+\Delta t} = \dot{\mathcal{U}}\}^{l, t} + a_6 \ddot{\mathcal{U}}\}^{l, t} + a_7 \mathcal{U}\}^{l, t+\Delta t},$$

where $a_0 = 1/(\alpha \Delta t^2)$, $a_2 = 1/(\alpha \Delta t)$, $a_3 = 1/2\alpha - 1$, $a_6 = \Delta t(1 - \beta)$, $a_7 = \beta \Delta t$, $\beta \geq 0.5$, $\alpha \geq 0.25(0.5 + \beta)^2$ are the conditions governing the stability of the integration scheme.

Let us consider the normal mode expansion method. Transformation to the normal coordinates is governed by the linear transformation

$$\mathcal{U}\}^{l, \tau} = [\Phi]_{lr} \{X\}_r^{l, \tau} \quad (r = 1, \dots, \Omega). \quad (13)$$

Here $\{X\}_r^l$ is the l th amplitude of the r th normal mode of the discrete model derived by modal analysis; $x_r(t)$ are the unknown weight coefficients obtained for the r th eigenmode; Ω is the number of the eigenmodes retained in the linear transformation.

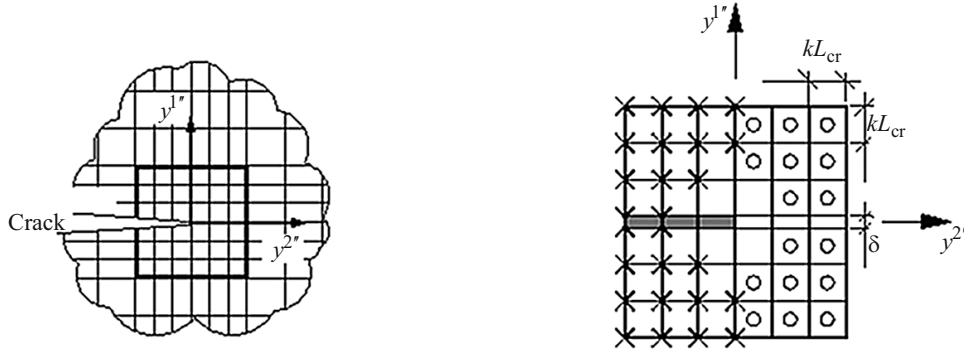


Fig. 4

Substitution (13) into (12) followed by the right multiplication by $[\Phi]_{lr}^T$ yields the system of equations that, in view of the orthogonality of eigenmodes

$$[\Phi]_{lr}^T [M]_{ll} [\Phi]_{lr} = [I]_{rr}, \quad [\Phi]_{lr}^T [K]_{ll} [\Phi]_{lr} = [\Lambda]_{rr},$$

can be reduced to the set of independent differential equation

$$[I]_{rr} \{\ddot{X}\}_r^{l,\tau} + [\Lambda]_{rr} \{X\}_r^{l,\tau} = [\Phi]_{lr}^T \{Q\}_r^{l,\tau}, \quad (14)$$

with the following initial conditions:

$$\{X_0\}_{r,Z^{i'}}^l = [\Phi]_{lr}^T [M]_{ll} \{U_0\}_{Z^{i'}}^l, \quad \{\dot{X}_0\}_{r,Z^{i'}}^l = [\Phi]_{lr}^T [M]_{ll} \{\dot{U}_0\}_{Z^{i'}}^l.$$

The solution of the 2-nd order ordinary differential equation (14) is represented by the Duhamel integral

$$\{X\}_r^{l,t} = [CC]^t \{X\}_r^{l,t_0} + [SS]^t \{\dot{X}\}_r^{l,t_0} + \int_{t_0}^t [SS]^{t-\tau} [\Phi]_{lr}^T \{Q\}_r^{l,\tau} d\tau,$$

where

$$[CC]^\tau = \text{diag}[\cos \theta_r \tau], \quad [SS]^\tau = \text{diag}\left[\frac{\sin \theta_r \tau}{\theta_r}\right], \quad \theta_r = \sqrt{\lambda_r}.$$

The rectangular integration formula is used for numerical integration.

Using formulas (2)–(7) and expansions (10) and (11), we derive the expression for the SIF amplitudes for each SAFEM subsystem:

$$K_\zeta^\sigma = \frac{\bar{\sigma}_l^{ij''} \Psi_{1'}^l + \bar{\sigma}_l^{ij''} \Psi_{3'}^l}{H_\zeta^{ij''}(r, \theta)}, \quad K_\zeta^u = \frac{u_i^l \Psi_{1'}^l}{H_\zeta^{i''}(r, \theta)}.$$

The coordinate values are calculated by the formulas

$$K_\zeta^\sigma = \sum_{l=l_0}^L K_\zeta^l, \quad K_\zeta^u = \sum_{l=l_0}^L K_\zeta^l, \quad \zeta = I, II, III.$$

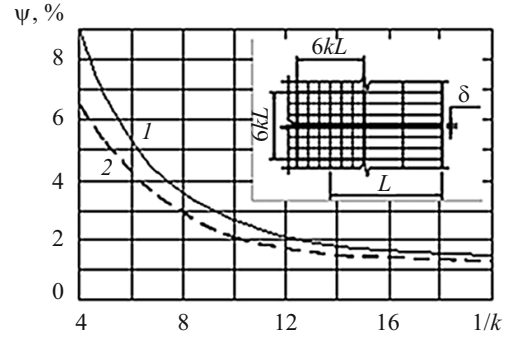
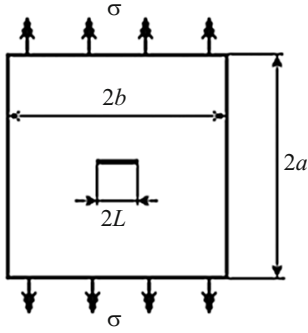


Fig. 5

The SIF is determined by averaging over a region of 6×6 elements (Fig. 4):

$$K_{\zeta} = \sum_{l=l_0}^L K_{\zeta}^l, \quad K_{\zeta}^l = \frac{1}{2} (K_{\zeta}^{\sigma l} + K_{\zeta}^u l),$$

where K^{σ} is the stress-based SIF while K^u is the displacement-based SIF. The points of determining the stress-based and displacement-based SIF are marked with circles and crosses, respectively.

Figure 5 shows the scheme of numerical analysis of the variation in the parameter k over the region adjacent to the crack surface. It corresponds to the above-mentioned SIF calculation technique. The solutions obtained are used to plot the accuracy ψ of the direct calculation of the SIF for the dynamic problem. The curve refines the optimal index of the FE dimension $k = 1/15 \dots 1/20$ as compared with the case of static loading [3].

Formulation (15) is traditionally used to calculate the energy integral within mesh methods. It is assumed that the coordinate system x^{α} is attached to the crack (Fig. 6), where the superscript α defines the direction along the crack; N_j are the sides of the integration contour chosen

$$\begin{aligned} & \sum_{j=1}^{N_3} (W+T)_{\alpha} ds_j - \sum_{j=1}^{N_1} (W+T)_{\alpha} ds_j - \sum_{j=1}^{N_1} (n_i \sigma^{ik} \zeta_{k\alpha}) ds_j \\ & - \sum_{j=1}^{N_2} (n_i \sigma^{ik} \zeta_{k\alpha}) ds_j - \sum_{j=1}^{N_3} (n_i \sigma^{ik} \zeta_{k\alpha}) ds_j - \sum_{j=1}^{N_4} (n_i \sigma^{ik} \zeta_{k\alpha}) ds_j. \end{aligned} \quad (15)$$

The force method [2] is applied in the present paper. According to it, all terms in (15) are defined by nodal forces and mesh domain displacements at moment $\tau = t + \Delta t$. The components in (15) can be expressed in terms of the amplitudes

$$\begin{aligned} (W^l + T^l) dS_j &= \frac{\{u\}_{lj}^T \{R\}_{lj}}{2(\Delta x_{\alpha})_j}, \quad R_{l2-4}^k = \frac{n_i \sigma_{l2-4}^{ik} dS}{2}, \quad R_{l1-3}^k = \frac{n_i \sigma_{l1-3}^{ik} dS}{2}, \\ R_{l2-4}^k &= \frac{1}{2} (R_{l2}^k + R_{l4}^k), \quad \zeta_{2-4}^{kl} = \left(\frac{\partial u_{li}}{\partial x^k} \right)_{2-4} = \frac{1}{\Delta x_{\alpha}} (u_{l4}^k - u_{l2}^k), \\ R_{l1-3}^k &= \frac{1}{2} (R_{l1}^k + R_{l3}^k), \quad \zeta_{1-3}^{kl} = \left(\frac{\partial u_{li}}{\partial x^k} \right)_{1-3} = \frac{1}{\Delta x_{\alpha}} (u_{l3}^k - u_{l1}^k). \end{aligned}$$

Finally, the expression can be written as

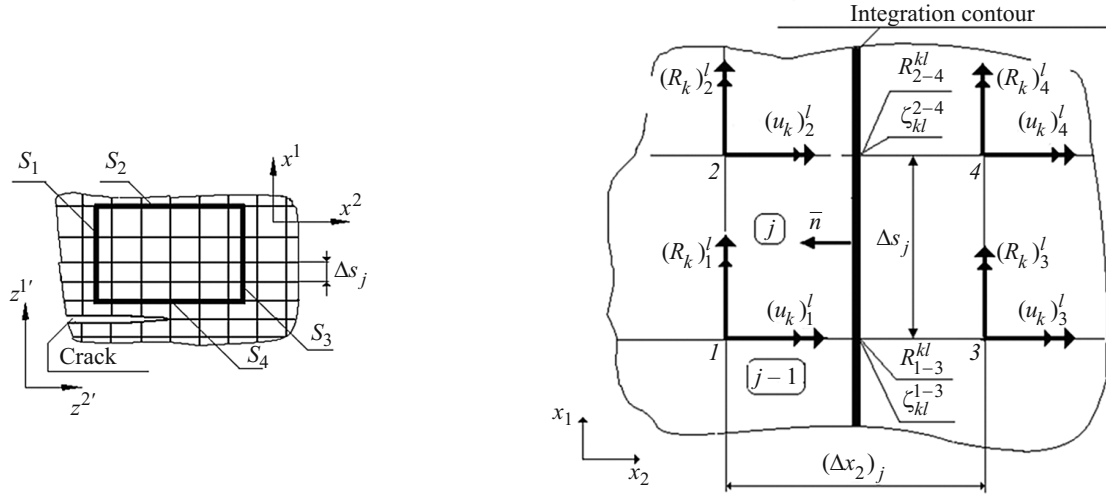


Fig. 6

$$\begin{aligned}
 & \sum_{j=1}^{N_3} \frac{1}{2(\Delta x_\alpha)_j} \{u\}_{lj}^T \{R\}_{lj} - \sum_{j=1}^{N_1} \frac{1}{2(\Delta x_\alpha)_j} \{u\}_{lj}^T \{R\}_{lj} \\
 & - \sum_{j=1}^{N_1} \left(\frac{(R_{lq}^k + R_{lq'}^k)(u_{lq}^k - u_{lq'}^k)}{2\Delta x_\alpha} \right)_j - \sum_{j=1}^{N_2} \left(\frac{(R_{lq}^k + R_{lq'}^k)(u_{lq}^k - u_{lq'}^k)}{2\Delta x_\alpha} \right)_j \\
 & - \sum_{j=1}^{N_3} \left(\frac{(R_{lq}^k + R_{lq'}^k)(u_{lq}^k - u_{lq'}^k)}{2\Delta x_\alpha} \right)_j - \sum_{j=1}^{N_4} \left(\frac{(R_{lq}^k + R_{lq'}^k)(u_{lq}^k - u_{lq'}^k)}{2\Delta x_\alpha} \right)_j.
 \end{aligned}$$

Formulas for calculation of the nodal force amplitudes depend on the algorithm of solving the equations of motion.

According to the Newmark scheme [4], the system of equations (12) can be rewritten as follows:

$$\{R_w\}_l^{t+\Delta t} + \{\bar{R}_p\}_l^{t+\Delta t} = \{Q\}_l^{t+\Delta t} + \{\bar{R}_p\}_l^t,$$

where

$$\{R_w\}_l^{t+\Delta t} = [K]_{ll} \{U\}_l^{t+\Delta t}, \quad \{\bar{R}_p\}_l^{t+\Delta t} = a_0 [M]_{ll} \{U\}_l^{t+\Delta t},$$

$$\{\bar{R}_p\}_l^t = [M]_{ll} a_0 \{U\}_l^{l,t} + a_2 \{\dot{U}\}_l^{l,t} + a_3 \{\ddot{U}\}_l^{l,t}.$$

Therefore, the nodal forces for the dynamic problem for a body with a crack in the case of direct integration of the equations of motion can be calculated as

$$\{R\}_l^\tau = \{R_w\}_l^{t+\Delta t} + \{\bar{R}_p\}_l^{t+\Delta t} - \{\bar{R}_p\}_l^t, \quad (16)$$

which contains both static and dynamic components.

It worth mentioning here that the dynamic component of force (16) is not unique for different methods (Wilson, Houbolt, etc.) of the direct integration of the equations of motion. It can be determined according to the method chosen.

If the dynamic solution of the problem is formed using the eigenmodes of structure, the nodal forces are calculated as follows:

$$\{R\}_l^\tau = \{R_w\}_l^\tau - \{\bar{R}_p\}_l^\tau,$$

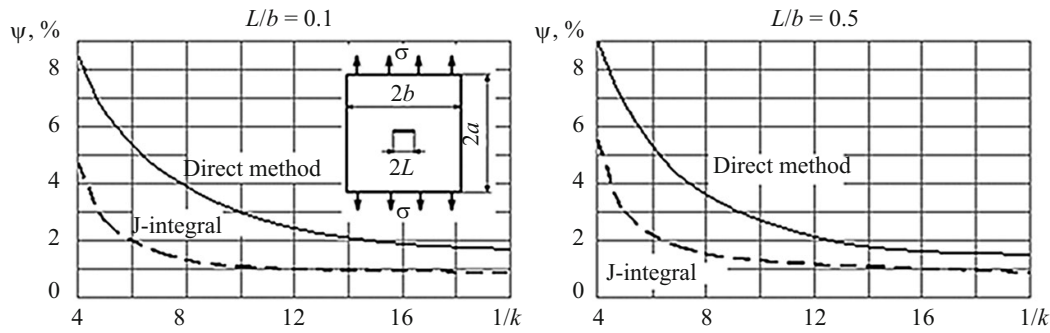


Fig. 7

where $\{R_w\}_l^\tau = [K]_{ll} \{U\}_l^{l,\tau}$, $\{R_p\}_l^\tau = \lambda_r [M]_{ll} \{U\}_l^{l,\tau}$.

Application of the method proposed to the problem of dynamic tension of a rectangular plate with a central crack provides good convergence of the calculation results (Fig. 7). Cracks of different length were studied. Results for two of them are presented in Fig. 7 as convergence curves with respect to the accuracy ψ of the SIF calculation.

It should be mentioned that the solution based on the force method converges much faster and allows for coarser meshing around the crack tip.

Conclusions. Based on the semi-analytical finite element method, the approach for studying linear fracture mechanics problems for dynamically loaded spatial bodies of revolution and prismatic bodies containing a crack has been developed.

A combination of a special finite element with crack as a model with direct correction of the stress tensor for ordinary FE and an algorithm of averaging the solutions over an effective near-the-tip subdomain has been proposed. It allows retaining the regularity of the discrete model structure and reducing the computational costs.

An approach to the evaluation of the energy integral for discrete SAFEM models has been elaborated based on the method of forces for dynamic problems.

REFERENCES

1. S. N. Atluri, *Computational Methods in the Mechanics of Fracture*, Elsevier Science Publishers, Amsterdam (1986).
2. V. A. Bazhenov, O. I. Gulyar, S. O. Piskunov, O. S. Sakharov, and O. O. Shkriil, "The force method for evaluation of J-integral in spatial nonlinear problems of fracture mechanics," *Sopr. Mater. Teor. Sooruzh.*, **79**, 3–17 (2006).
3. V. A. Bazhenov, A. I. Gulyar, A. S. Sakharov, and A. G. Topor, *Semianalytic Finite Element Method in Solid Mechanics* [in Russian], Vipol, Kiev (1993).
4. K. J. Bathe and E. L. Wilson, *Numerical Methods in Finite Element Analysis*, Prentice Hall, Englewood Cliffs, N. J. (1976).
5. V. I. Blokh, *Theory of Elasticity* [in Russian], Izdat. Kharkov Univ., Kharkov (1964).
6. O. S. Zienkiewicz, *The Finite Element Method in Engineering Science*, McGraw-Hill, London (1972).
7. A. B. Zolotov, *Discrete-Continuous Finite Element Method. Civil Engineering Applications* [in Russian], ACB, Moscow (2010).
8. B. Ya. Kantor and V. I. Gnitko, "On a method for the analysis of the strain state of thin-wall structures of revolution that are cyclically inhomogeneous along the circumference," *IPMash AN USSR*, Kharkov, preprint 171 (1982).
9. E. M. Morozov and G. P. Nikishkov, *Finite Element Method in Fracture Mechanics* [in Russian], Nauka, Moscow (2007).
10. A. N. Guz (ed.), *Nonclassical Problems of Fracture Mechanics* [in Russian], four volume series, Naukova Dumka, Kiev (1993).
11. M. P. Savruk, *Fracture Mechanics and Strength of Materials. Handbook. Vol. 2, Stress Intensity Factors in Solids with Cracks*, Naukova Dumka, Kiev (1988).

12. I. I. Solodei, "Efficiency of SAFEM finite element basis for approximation of bodies of revolution and prismatic bodies in dynamic problems," *Sopr. Mater. Teor. Sooruzh.*, **82**, 154–163 (2008).
13. G. P. Cherepanov, *Mechanics of Brittle Fracture*, McGraw-Hill, New York (1979).
14. A. A. Kotlyarenko, T. A. Prach, V. V. Kharchenko, and A. Yu. Chirkov, "Numerical simulation of stress–strain state near crack tip in a compact tensile specimen," *Strength of Materials*, **41**, No. 1, 106–112 (2009).
15. V. L. Bogdanov, A. N. Guz, and V. M. Nazarenko, "Spatial problems of the fracture of materials loaded along cracks (review)," *Int. Appl. Mech.*, **51**, No. 5, 3–89 (2015).
16. J. Rice, "A path independent integral and the approximate analysis of strain concentrations by notches and cracks," *J. Appl. Mech.*, **35**, No. 2, 379–386 (1968).